

Engineered Nanomembranes for Directing Cellular Organization Toward Flexible Biodevices

Toshinori Fujie,[†] Samad Ahadian,[†] Hao Liu,[†] Haixin Chang,[†] Serge Ostrovidov,[†] Hongkai Wu,[†] Hojae Bae,[‡] Ken Nakajima,[†] Hirokazu Kaji,[§] and Ali Khademhosseini^{*,†,||,⊥,¶}

[†]WPI-Advanced Institute for Materials Research (WPI-AIMR), Tohoku University, 2-1-1 Katahira, Aoba-ku, Sendai, 980-8577, Japan

[‡]College of Animal Bioscience and Technology, Department of Bioindustrial Technologies, Konkuk University, Hwayang-dong, Kwangjin-gu, Seoul 143-701, Republic of Korea

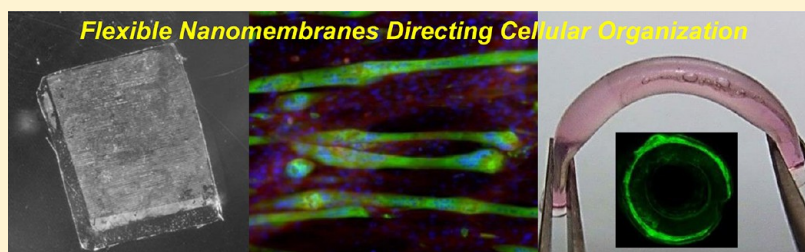
[§]Department of Bioengineering and Robotics, Graduate School of Engineering, Tohoku University, 6-6-01 Aramaki, Aoba-ku, Sendai 980-8579, Japan

^{||}Center for Biomedical Engineering, Department of Medicine, Brigham and Women's Hospital, Harvard Medical School, Harvard University, Cambridge, Massachusetts, United States

[⊥]Harvard-MIT Division of Health Sciences and Technology, Massachusetts Institute of Technology, Cambridge, Massachusetts, United States

[¶]Wyss Institute for Biologically Inspired Engineering, Harvard University, 02139, PRB-252, 65 Landsdowne Street, Cambridge, Massachusetts, United States

Supporting Information



ABSTRACT: Controlling the cellular microenvironment can be used to direct the cellular organization, thereby improving the function of synthetic tissues in biosensing, biorobotics, and regenerative medicine. In this study, we were inspired by the microstructure and biological properties of the extracellular matrix to develop freestanding ultrathin polymeric films (referred as “nanomembranes”) that were flexible, cell adhesive, and had a morphologically tailorable surface. The resulting nanomembranes were exploited as flexible substrates on which cell-adhesive micropatterns were generated to align C2C12 skeletal myoblasts and embedded fibril carbon nanotubes enhanced the cellular elongation and differentiation. Functional nanomembranes with tunable morphology and mechanical properties hold great promise in studying cell–substrate interactions and in fabricating biomimetic constructs toward flexible biodevices.

KEYWORDS: Nanomembranes, nanomechanical properties, extracellular matrix, carbon nanotubes, skeletal muscle cells

Directing cellular organization is important for the development of various synthetic tissues in biosensing, biorobotics, and regenerative medicine. To this end, there have been significant efforts in recreating tissue structure by combining materials with nano- or microscale technologies.¹ Extracellular matrix (ECM) in native tissues has an ideal structure and function to direct the cellular organization and therefore to regenerate and maintain tissues and organs.² To mimic the ECM, topographically and mechanically tailored structures have been created by using polymeric materials, microfabrication techniques and functional nanomaterials (e.g., nanofibers, nanowires, or nanotubes), which direct cellular organization and induce tissue formation.³ Materials, such as hydrogels and elastomers have been employed as cellular scaffolds owing to their tailorable structures and tunable

mechanical properties.⁴ Recent studies suggest that the incorporation of nanomaterials in such scaffolds can be used to further enhance their desirable mechanical, biological, chemical, and electrical properties.⁵ In addition, freestanding cell sheets were fabricated by utilizing thermoresponsive cell culture dishes and stacked to generate a quasi three-dimensional multilayered structure.⁶ Such technology may be useful to assemble different properties of the cellular sheets into hierarchical structures. ECM is made from nanofibrous structures (e.g., structural proteins and polysaccharides)

Received: April 6, 2013

Revised: May 26, 2013

Published: June 11, 2013

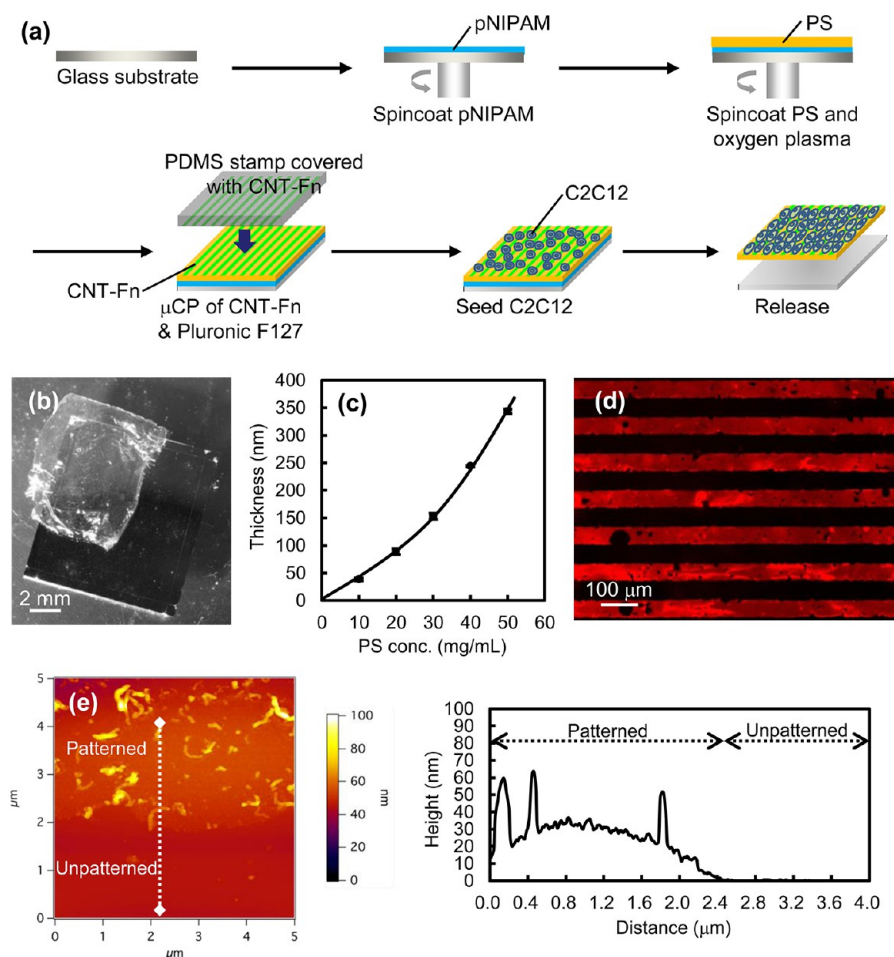


Figure 1. Preparation of nanomembranes with micropatterned CNT-Fn nanocomposite. (a) Schematic of nanomembranes with aligned C2C12 myoblasts. (b) Macroscopic image of the freestanding nanomembrane with CNT-Fn micropatterns in PBS released from the silicon substrate (40 nm thick, $1 \times 1 \text{ cm}^2$). (c) Thickness profile of the nanomembranes as a function of polymer concentration. (d) Fluorescent image of CNT-Fn micropatterns on the nanomembrane (Fn labeled with rhodamine). (e) AFM images of CNT-Fn micropatterns and height measurement along the dashed line.

containing numerous types of cell adhesive domains (e.g., collagen, laminin, fibronectin, vitronectin, and elastin).² Thus, it is challenging to recreate the natural complexity of ECM in miniaturized engineered structures that aim to build functional tissue structures.

Ultrathin polymeric films are a new class of polymeric nanomaterials, conventionally studied in polymer physics field.⁷ These films are typically tens of nanometers in thickness and have unique interfacial and mechanical properties, which are unlike bulk polymeric materials. For example, their thermodynamic properties (particularly, glass transition temperature) are controlled in a thickness-dependent manner, resulting in tunable mechanical property, noncovalent adhesiveness, and selective molecular permeability.⁸ Such properties are beneficial for various applications, including as wound dressings,⁹ filtration membranes,¹⁰ and optoelectronics sensors.¹¹ Previously, we demonstrated that the large surface area of the ultrathin films was beneficial to create a flexible substrate with thickness-dependent mechanical properties, which directed the adhesion morphology of cardiomyocytes in a stiffness dependent manner.¹² The surface morphology of these nanomembranes can also be tailored by the integration of nanomaterials (e.g., nanoparticles),¹³ which may enhance the morphological guidance of the cells.¹⁴ Thus, we hypothesized

that a quasi two-dimensional structure of such ultrathin films may be useful as synthetic mimics of the natural basement membrane in ECM, which has an amorphous, dense, sheetlike structure of 50–100 nm in thickness.¹⁵ Herein, we attempted to recapitulate the ECM properties (such as flexibility, cell adhesiveness, and nanostructure) on the ultrathin polymeric films toward the development of functional nanomembranes for use as flexible biodevices. Specifically, we made flexible freestanding nanomembranes, and functionalized them with cell adhesive proteins by microcontact printing (μ CP). We utilized the large surface area of the nanomembrane and embedded multiwalled carbon nanotubes (CNTs) in cell-adhesive micropatterns as nanoscale cues to control the cellular morphology since diameter of CNT (around 100 nm) is close to the size of the cellular filopodia.¹⁶ On these nanomembranes, we seeded C2C12 skeletal myoblasts and evaluated the effect of the tailored surfaces on myofiber formation, through analyzing myoblast alignment and myotube formation. Such a flexible structure was exploited for directing the cellular organization as well as engineering the biomimetic constructs (e.g., tubular structure), which may be exploited as a unique template to build lab-on-a-chip devices. For instance, the flexible structure can be shaped and integrated into the silicone-based soft devices (e.g., microfluidics) to fabricate biomimetic structure,¹⁷

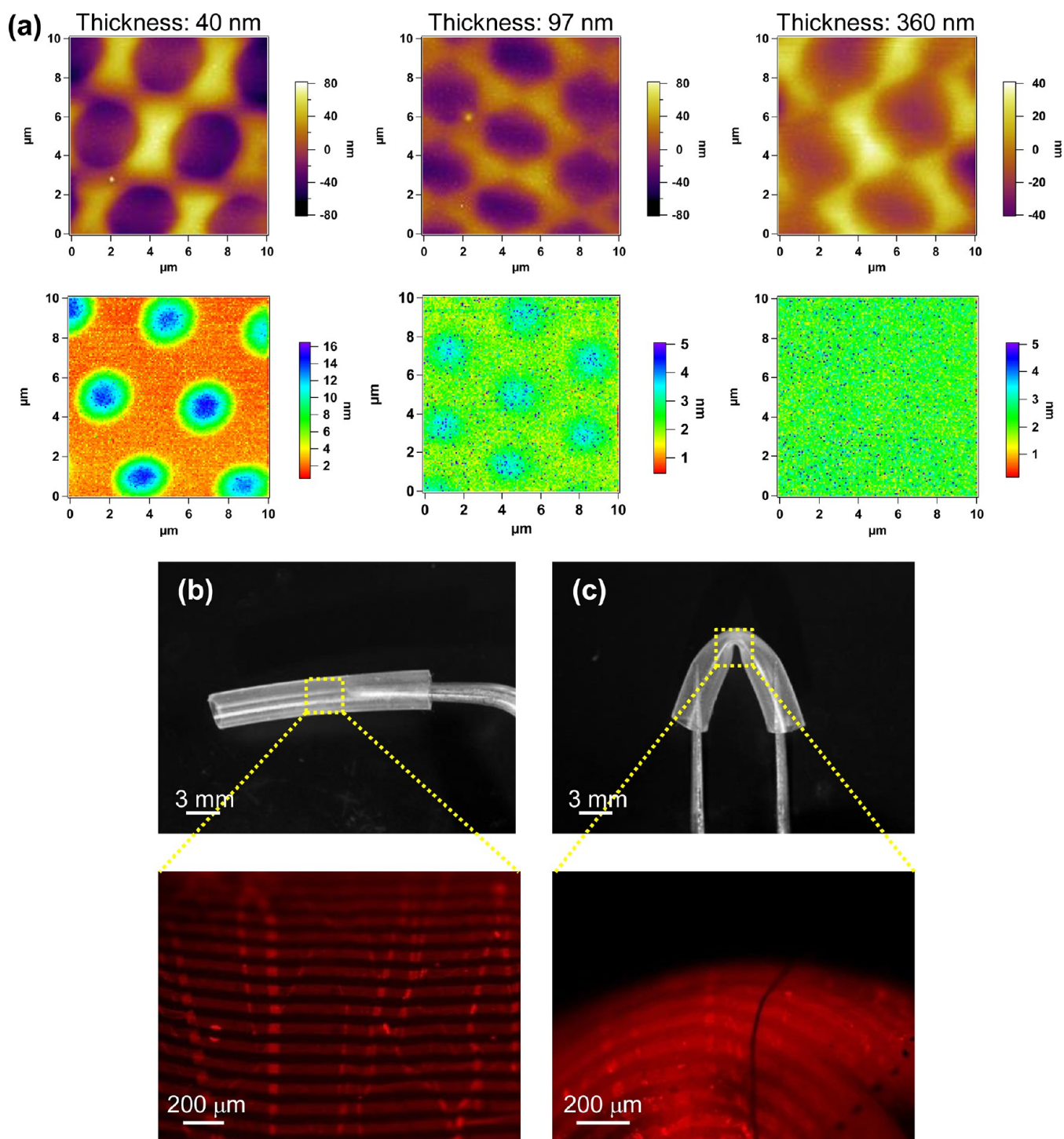


Figure 2. Mechanical properties of the nanomembranes. (a) Nanomechanical analysis of freestanding PS nanomembranes suspended on a honeycomb film ($3 \mu\text{m}$ ϕ): height (top) and deformation (bottom) maps for different thicknesses. Macroscopic and magnified fluorescent images of the nanomembranes (40 nm thick) wrapping a silicone tube ($3 \mu\text{m}$ ϕ) (b) before and (c) after bending the tube. The micropatterns (rhodamine labeled fibronectin) were flexible and adhered to the curvature of the tube in the bending state.

which may be useful as flexible biodevices to evaluate tissue response to various drugs and toxic chemicals.¹⁸

We employed polystyrene (PS) to generate the nanomembranes, due to its manufacturability, well-known physical properties, ease of surface modification, as well as its long history of use in cell culture applications. Nonetheless, in the future PS may also be substituted with other types of materials that are more commonly used in tissue engineering. The PS-

based nanomembranes were fabricated by combining spincoating and μCP techniques (Figure 1a). Initially, an ultrathin polymeric film was prepared by spincoating PS ($M_w \sim 280\,000$) on a glass substrate covered with a temperature-responsive sacrificial layer composed of poly(*N*-isopropylacrylamide) (pNIPAM). Thus, the dissolution of the pNIPAM layer under lower critical solution temperature (32°C) allowed for the release of nanomembrane (Figure 1b). The film thickness

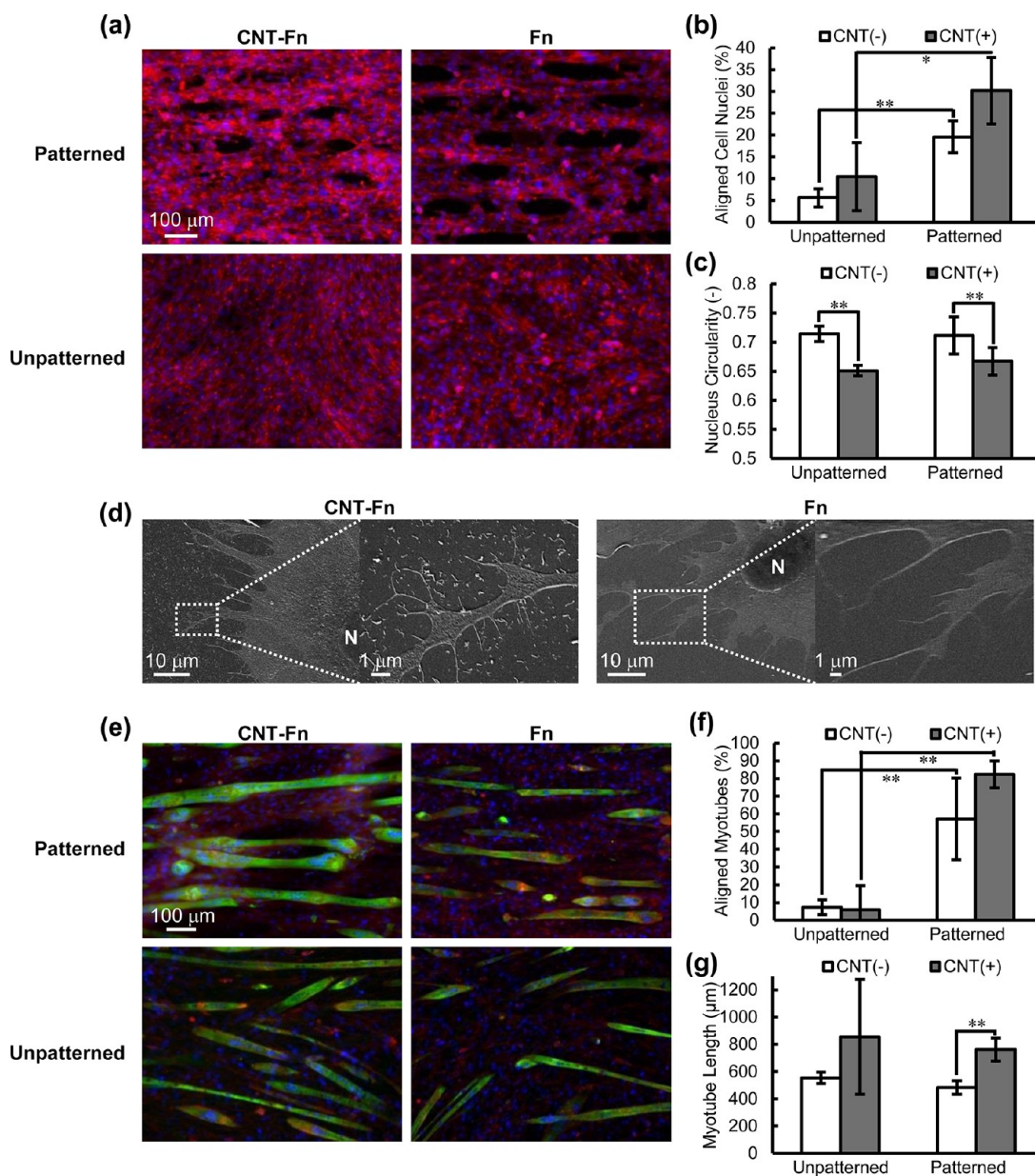


Figure 3. Influence of CNT-Fn nanocomposite on myoblast adhesion (24 h) and myotube formation on the nanomembranes (8 days in differentiation medium). (a) Immunofluorescent images of nucleus (blue) and F-actin (red) for patterned CNT-Fn, patterned Fn, unpatterned CNT-Fn and unpatterned Fn surfaces. Quantification of (b) cell nucleus alignment (between 0 and 10°) and (c) circularity on patterned and unpatterned CNT-Fn/Fn nanomembranes, respectively. (d) SEM images of myoblasts on different surface properties of the nanomembranes: CNT-Fn and Fn surface with magnified images (letter “N” indicates nucleus). Pseudopodia on the CNT-Fn surface spread more branched filopodia than those on the Fn surface. (e) Immunofluorescent images of myosin heavy chains (green), nucleus (blue), and F-actin (red) for patterned CNT-Fn, patterned Fn, unpatterned CNT-Fn and unpatterned Fn surface. Quantification of (f) myotube alignment (between 0 and 10°), and (g) myotube length on patterned and unpatterned CNT-Fn/Fn nanomembranes, respectively. Student’s *t* test with $^{**}p < 0.01$ and $^{*}p < 0.05$ set as the level of statistical significance.

was controlled by the function of polymer concentration from tens to hundreds of nanometers in thickness (Figure 1c). We then prepared cell-adhesive micropatterns on the nanomembrane using μ CP to functionalize the film surface to organize the cells. In this step, we also incorporated CNTs in the fibronectin (Fn) micropatterns since the rigid and fibrous structure of CNTs would provide mechanical cues for cells. Herein, we expect the synergistic effect of biological adhesion (by micropatterned Fn) and nanoscale structural guidance (by CNTs) toward controlling the cellular activities on the nanomembranes. The CNT-Fn nanocomposite was prepared

by mixing Fn into CNT solution (approximately 1 mg/mL) at the final concentration of 50 μ g/mL (see detailed characterizations in Supporting Information Figure S1). The CNT-Fn nanocomposite was micropatterned on the nanomembrane after surface hydrophilization by oxygen plasma. The μ CP process was performed by using poly(dimethyl siloxane) (PDMS) molds with microscopic groove-ridge features of 50 μ m width and 50 μ m separation since it was shown that myotube alignment was enhanced on cell-adhesive micropatterns that were less than 100 μ m wide.¹⁹ Then, the unpatterned regions were rendered cytophobic by Pluronic F-

127 to promote the initial cell alignment. The μ CP process resulted in the preparation of spatially controlled micropatterns on the nanomembrane (Figure 1d) on which we observed homogeneous distribution of CNT-Fn nanocomposites with variation in height (Figure 1e).

One of the important physical properties of the freestanding nanomembrane is thickness-dependent mechanical dynamics.²⁰ To detail the mechanical properties of the freestanding nanomembrane, we analyzed the nanomechanical properties of the nanomembranes by using atomic force microscopy (AFM).²¹ With this technique, quantitative mechanical mapping with on-site morphology can be acquired simultaneously to investigate the topographical and mechanical properties of the nanomembranes. Therefore, nanomechanical mapping is a valuable method to evaluate the microscopic surface properties of soft materials.²² We used honeycomb-like porous PS films with periodically aligned 3 μ m holes (referred as “honeycomb films”²³) to suspend the freestanding nanomembrane on a surface. This setup allowed us to clarify the mechanical property of the freestanding nanomembranes by the function of the thickness. As we scanned the surface of nanomembranes with different thicknesses (40, 97, and 360 nm) (Figure 2a), we found that 40 nm thick nanomembrane showed a larger deformation than that of the 360 nm thick nanomembrane at the same trigger force (3.26 nN). Interestingly, deformation of the nanomembrane was already detected at 97 nm thickness, which has a similar trend to the mechanical property of amorphous PS ultrathin films with tens of nanometers thickness.²⁴ Indeed, the critical thickness of the nanomembrane with large displacement (40 nm thick) is close to twice of the radius of gyration of a PS chain (around 30 nm for 300 kDa).²⁵ This reflects a specific interfacial property of the ultrathin film, such as unrestricted polymer chain mobility inside structures²⁶ and is probably the reason why the present PS nanomembranes have a higher flexibility than the corresponding bulk PS films.

The nanomechanical mapping revealed that the PS nanomembranes with different thicknesses showed variable deformation length at the same indentation force, which could be useful in designing flexible nanomembranes for wrapping and tailoring the biodevice surface. It is noteworthy that the film deformation is dominated by both the bending deflection of freestanding nanomembranes under load, as well as the local indentation of nanomembranes by the cantilever tip. Thus, the Young's modulus of the nanomembranes can be calculated by combining these two factors. Future studies aim to determine the Young's modulus by integrating the appropriate theoretical models in order to compare the values with other tissue engineering matrices. Importantly, our findings highlight the high flexibility of freestanding nanomembranes by simply decreasing the film thickness, which is applicable as “ultrathin stickers”. For example, a silicone tube (3 mm diameter) was wrapped by a 40 nm thick freestanding nanomembrane with CNT-Fn micropattern (Figure 2b). Despite bending the tube by tweezers, the micropattern alignment was retained owing to the physical adhesiveness and flexibility of nanomembrane (Figure 2c). In addition, the 40 nm thick nanomembrane showed stable adhesion on the tube wall, while the 360 nm one showed corrugation and partial detachment from the corner when put in water (data not shown). Such unique mechanical properties of the nanomembrane can be used for tailoring and functionalizing the

surface of a silicone-based device, which may be a convenient tool to control the behavior of anchorage-dependent cells.

Next, we exploited the large surface of the nanomembrane, and evaluated the effect of the CNT-Fn micropatterns on cellular morphology using murine skeletal myoblasts (C2C12) since surface structure is an important factor to direct the morphogenesis of myoblasts and myotubes.¹⁹ After 24 h of cell seeding, we observed the anisotropic alignment of C2C12 myoblasts both on the CNT-Fn and Fn micropatterned surfaces, while randomly oriented cells were observed both on the CNT-Fn and Fn unpatterned surfaces (Figure 3a). Then, the cell nucleus alignment was quantified along the micropatterns to assess the myoblast alignment in the horizontal direction. Consistent with the fluorescent images, nucleus alignment quantification indicated that the myoblasts significantly aligned on both micropatterns (Figure 3b). The degree of nucleus alignment on the CNT-Fn micropatterns (ca. 30%) was slightly higher than that on the Fn micropatterns (ca. 20%) (Supporting Information Figure S2). We also evaluated the nucleus shape index (referred as “nucleus circularity”). It is known that a decrease on the circularity of the cells over time implies a tendency to elongate.²⁷ We found that the myoblasts on the CNT-Fn surfaces showed significant elongation, independent from the surface texture (Figure 3c, $p < 0.01$). From SEM images, we confirmed that the myoblasts adhered to the CNT-Fn nanocomposite embedded surface with spread pseudopodia (Figure 3d). Interestingly, pseudopodia on the CNT-Fn surface had more branched filopodia than those on the Fn surface. Such structural effect by CNT was confirmed in previous reports using bulk CNT scaffolds.²⁸ Therefore, it is suggested that CNT inside the Fn matrix induced mechanotaxis of C2C12 myoblasts. Taking account the cellular behavior above, existence of the CNT-Fn nanocomposite enhanced not only the elongation of the cells but also the overall alignment of the myoblasts along the micropattern. These results are in agreement with a recent report, where it was shown that micropatterned CNT surfaces enhanced filopodial growth of NIH3T3 fibroblasts or mesenchymal stem cells.²⁹

We also investigated myotube formation on the nanomembranes since myotube alignment is crucial for maximizing the contractility of muscle tissue.³⁰ After 8 days in differentiation medium, the formation of C2C12 myotubes was confirmed by immunostaining of myosin heavy chain. We observed aligned C2C12 myotubes both on CNT-Fn and Fn micropatterned surfaces, while, random alignment was observed both on CNT-Fn and Fn unpatterned surfaces (Figure 3e). The quantification of myotube alignment showed higher degree of the myotube alignment on both micropatterned surfaces (Figure 3f). Notably, the distribution of myotube orientation was shifted from ≤ 30 degrees (Fn micropattern) to ≤ 20 degrees (CNT-Fn micropattern) (Supporting Information Figure S3), which suggested that CNT-Fn micropattern promoted the formation of highly organized synthetic myofibers. We also found that the averaged myotube length on CNT-Fn micropatterned surfaces was significantly more than that on Fn micropatterned surfaces (Figure 3g, $p < 0.01$). The greater alignment of the myoblasts promoted end-to-end connection with each other, and therefore favored the assembly of myotubes during the differentiation process. Correspondingly, electrical stimulation induced the myotube contraction after 6 h, where we found that C2C12 myotubes on CNT-Fn surfaces showed larger

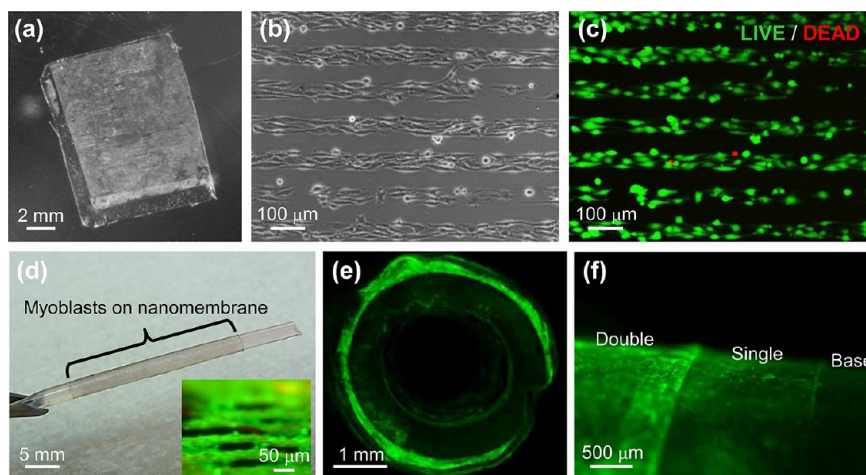


Figure 4. Biomimetic cellular organizations directed by the nanomembranes. (a) Macroscopic image of the freestanding nanomembrane with micropatterned C2C12 myoblasts ($1 \times 1 \text{ cm}^2$). (b) Phase contrast and (c) fluorescent images of aligned myoblasts on the nanomembranes, analyzed by live/dead staining after 24 h of culture. (d) Macroscopic image of the rolled myoblasts on the nanomembrane ($2 \times 2 \text{ cm}^2$) around a silicone tube ($3 \text{ mm } \varnothing$) (Inset: myoblast micropatterns on the tube surface stained by calcein AM). (e) Fluorescent images of rolled myoblast construct and (f) layered structure wrapped approximately twice around the tube (stained by CellTracker Green CMFDA).

displacement and contractility than those on Fn surfaces (see Supporting Information Supplementary Movies).

Finally, we utilized the freestanding nanomembrane as an ultrathin flexible substrate for building biomimetic cellular constructs. Tissues with tubular structure such as blood vessels and intestinal tracts have distinguished function originated from their structure, represented by the controlled flux of blood or nutrients. In particular, the blood vessel has a specific structure consisting of multilayered smooth muscle cells with anisotropic alignment around the endothelialized layer. Thus, the recapitulated muscular structure may be a good model of the artery wall to study physiology and dysfunction of the blood vessels.¹⁷ In this regard, the tubular structure mediated by the flexible nanomembrane could be used for mimicking the natural tissue arrangement, which may facilitate the engineering of drug-screening devices. Thus, we demonstrated how to generate artificial tubular structure consisting of the myoblasts cultured on the micropatterned nanomembrane. It can be fabricated by simply rolling the cell/nanomembrane construct around the template while keeping the cellular alignment. After one day of culture, we released the nanomembrane bearing micropatterned myoblasts by dissolution of pNIPAM (Figure 4a). Myoblasts aligned anisotropically along the CNT-Fn micropattern (Figure 4b) and remained viable (Figure 4c). The freestanding cell/nanomembrane construct was used to produce tubular structure by wrapping it around a template (e.g., silicone tube, 3 mm diameter) (Figure 4d). Although such wrapping process to engineer multilayered tissue structures has been recently proposed,³¹ they employed PDMS thin films that were more than $10 \mu\text{m}$ thick. Therefore, there is always a thick barrier between the cells on the neighboring sheets. By contrast, the cross-sectional image of the rolled myoblasts on nanomembrane ($2 \times 2 \text{ cm}^2$) showed a tightly wrapped structure surrounding the outer wall of the silicone tube (Figure 4e). From the lateral image, we also confirmed fluorescent signals of layered myoblasts due to the esterase activity of the myoblasts (Figure 4f). The results suggest that the freestanding nanomembrane serve as a synthetic basement membrane to engineer hierarchical cellular organization. Such a spatially unconfined structure of the flexible nanomembrane

can be shaped and integrated into the microfluidic system to study the function of synthetic tissues.

There have been ongoing efforts to recreate the ECM microenvironment to direct cellular organization for the development of cell-containing biodevices. For example, hydrogels can be used to modulate the physical and topographical properties by tuning the cross-linking density and tailoring their microarchitecture.²⁷ Alternatively, elastomers, such as PDMS have been used as flexible two-dimensional platforms.³² Nonetheless, the miniaturization and functionalization of synthetic substrates is beneficial to engineer the hierarchical cellular organizations. The present study showed the utility of freestanding nanomembranes as ultrathin and flexible synthetic basement membranes. The engineered nanomembrane exhibited high functionality as to give morphological guidance to the myoblasts for the maturation of synthetic myofibers. Indeed, it was confirmed that the dispersed CNT-Fn nanocomposite on the micropattern influenced the filopodial extension. The present finding can be used to design nanostructured surfaces to direct cellular morphology as well as generate complex tissue structures. Although we exploited morphological properties of CNT in this study, electrical properties could also be expected to enhance local electrical stimulation of muscle tissues as well as cell–cell communication for biosensing application.³³ Furthermore, the substitution of micropatterned CNT to other conductive materials (e.g., nanowires³⁴ or conductive polymers³⁵) may be used to further modulate cell–substrate interactions on the nanomembrane.

Our current study employed PS as a material source (because of its well-known physical properties that make it compatible for biodevice applications); however, biopolymers such as polylactides and polysaccharides can be applicable as material sources to engineer functional and biodegradable nanomembranes by employing other preparative techniques of the ultrathin films.^{36,37} For example, layer-by-layer (LbL) assembly will be an useful method for tuning the physicochemical property of the ultrathin films by changing thickness or cross-linking density.^{37,38} Such arrangement is beneficial for tailoring the properties of the nanomembranes (e.g., stiffness, perme-

ability, biodegradability). In particular, the higher stiffness may improve the mechanical property of the synthetic tissues such as blood vessels against the high-shear stress condition under arterial blood flow. The permeable property will be used for the fabrication of semipermeable membranes equipped with implantable dialyzers or drug release devices, allowing the controlled release of nutrients and drugs. In addition, biodegradable membranes will enhance the use of this approach for regenerative medicine as synthetic basement membranes. Also, to further enable the formation of 3D tissues, microscopic pores can be generated inside the nanomembrane by utilizing self-organization of polymers.³⁹ Such structures will allow for the close contact of layered cells on the nanomembrane through the pores, which will enhance cell–cell interactions and electrical coupling. Thus, the freestanding nanomembrane may be integrated into the multilayered cellular sheets,⁶ which direct the cellular organization and enhance the tissue formation *in vivo*. Therefore, the flexible nanomembranes hold great promise for various biomedical applications.

In summary, we developed functional nanomembranes with tens of nanometers in thickness as synthetic mimics of the ECM basement membrane that are flexible, cell-adhesive, and had a morphologically tailorable surface. Nanomechanical mapping revealed the high flexibility of engineered nanomembranes by simply decreasing the film thickness, which was applied as “ultrathin stickers” for tailoring the material surface. Then, the cell-adhesive micropatterns on the nanomembrane allowed for the alignment of C2C12 myoblasts, and embedded fibril CNTs enhanced the cellular elongation and differentiation to generate functional myofibers. The results suggest that the nanomembrane surface is a useful platform to study cell–substrate interaction. Furthermore, the flexible structure of cell/nanomembrane construct was utilized to generate the biomimetic tubular structure by simply rolling it around the template. The process will be useful for mimicking the blood vessel or intestinal structure, which may be integrated in lab-on-a-chip devices for the recapitulation of tissue dysfunction and the investigation of tissue response to various drugs and toxic chemicals. The freestanding nanomembrane will be a useful tool to direct the cellular organization and engineer the hierarchically assembled tissue structure toward the development of flexible biodevices and regenerative medicine applications.

■ ASSOCIATED CONTENT

● Supporting Information

Materials and Methods, detailed materials characterizations, and Supplementary Movies. This material is available free of charge via the Internet at <http://pubs.acs.org>.

■ AUTHOR INFORMATION

Corresponding Author

*E-mail: alik@rics.bwh.harvard.edu. Phone: (+1 617 7688395). Fax: (+1 617 7688477).

Author Contributions

T.F. and A.K. conceived of the project. H.L. helped for the AFM measurements with the K.N. supervision. H.C. synthesized and characterized CNTs with the H.W. supervision. T.F. designed and performed all other experiments, analyzed the results, and wrote the manuscript. S.A. edited the manuscript, performed the quantification parts, and analyzed

the results. S.O., H.B., and H.K. supervised the manuscript preparation. A.K. supervised the whole project.

Notes

The authors declare no competing financial interest.

■ ACKNOWLEDGMENTS

The authors thank Professor Matsuhiko Nishizawa (Department of Bioengineering and Robotics, Graduate School of Engineering, Tohoku University) for providing the lithography facilities, and also thank Dr. Jianli Kang and Professor Mingwei Chen (WPI-AIMR, Tohoku University) for the SEM analysis. The authors also acknowledge Dr. Yuji Hirai and Professor Masatsugu Shimomura (WPI-AIMR, Tohoku University) for providing the honeycomb films, Dr. Yasufumi Nakamichi for taking macroscopic images of the nanomembranes, and Dr. S. Prakash Parthiban for useful discussions through the project. This work was supported by the World Premier International Research Center Initiative (WPI) and JSPS KAKENHI (Grant 25870050 for T.F.) from MEXT, Japan.

■ REFERENCES

- (1) Khademhosseini, A.; Langer, R.; Borenstein, J.; Vacanti, J. P. *Proc. Natl. Acad. Sci. U.S.A.* **2006**, *103*, 2480–7.
- (2) Fernandes, H.; Moroni, L.; van Blitterswijk, C.; de Boer, J. J. *Mater. Chem.* **2009**, *19*, 5474–84.
- (3) Bettinger, C. J.; Langer, R.; Borenstein, J. T. *Angew. Chem., Int. Ed.* **2009**, *48*, 5406–15.
- (4) Slaughter, B. V.; Khurshid, S. S.; Fisher, O. Z.; Khademhosseini, A.; Peppas, N. A. *Adv. Mater.* **2009**, *21*, 3307–29.
- (5) Shin, S. R.; Jung, S. M.; Zalabany, M.; Kim, K.; Zorlutuna, P.; Kim, S. B.; Nikkhah, M.; Khabiry, M.; Azziz, M.; Kong, J.; Wan, K. T.; Palacios, T.; Dokmeci, M. R.; Bae, H.; Tang, X. S.; Khademhosseini, A. *ACS Nano* **2013**, *7*, 2369–80.
- (6) Haraguchi, Y.; Shimizu, T.; Sasagawa, T.; Sekine, H.; Sakaguchi, K.; Kikuchi, T.; Sekine, W.; Sekiya, S.; Yamato, M.; Umezumi, M.; Okano, T. *Nat. Protoc.* **2012**, *7*, 850–8.
- (7) Forrest, J. A.; Dalnoki-Veress, K. *Adv. Colloid Interface Sci.* **2001**, *94*, 167–96.
- (8) Fujie, T.; Okamura, Y.; Takeoka, S. In *Functional Polymer Films*; Knoll, W., Advincula, R. C., Eds.; Wiley-VCH: Weinheim, Germany, 2011; Vol. 2, p 907.
- (9) Fujie, T.; Okamura, Y.; Takeoka, S. *Adv. Mater.* **2007**, *19*, 3549–53.
- (10) Fujie, T.; Kawamoto, Y.; Haniuda, H.; Saito, A.; Kabata, K.; Honda, Y.; Ohmori, E.; Asahi, T.; Takeoka, S. *Macromolecules* **2013**, *46*, 395–402.
- (11) Huang, G.; Mei, Y. *Adv. Mater.* **2012**, *24*, 2517–46.
- (12) Fujie, T.; Ricotti, L.; Desii, A.; Menciassi, A.; Dario, P.; Mattoli, V. *Langmuir* **2011**, *27*, 13173–82.
- (13) Taccola, S.; Desii, A.; Pensabene, V.; Fujie, T.; Saito, A.; Takeoka, S.; Dario, P.; Menciassi, A.; Mattoli, V. *Langmuir* **2011**, *27*, 5589–95.
- (14) Fujie, T.; Furutate, S.; Niwa, D.; Takeoka, S. *Soft Matter* **2010**, *6*, 4672–6.
- (15) Yurchenco, P. D. *Cold Spring Harbor Perspect. Biol.* **2011**, *3*, a004911.
- (16) Correa-Duarte, M. A.; Wagner, N.; Rojas-Chapana, J.; Morszeck, C.; Thie, M.; Giersig, M. *Nano Lett.* **2004**, *4*, 2233–6.
- (17) Günther, A.; Yasotharan, S.; Vagaon, A.; Lochovsky, C.; Pinto, S.; Yang, J.; Lau, C.; Voigtlaender-Bolz, J.; Bolz, S.-S. *Lab Chip* **2010**, *10*, 2341–9.
- (18) Huh, D.; Matthews, B. D.; Mammoto, A.; Montoya-Zavala, M.; Hsin, H. Y.; Ingber, D. E. *Science* **2010**, *328*, 1662–8.
- (19) Hosseini, V.; Ahadian, S.; Ostrovidov, S.; Camci-Unal, G.; Chen, S.; Kaji, H.; Ramalingam, M.; Khademhosseini, A. *Tissue Eng., Part A* **2012**, *18*, 2453–65.

- (20) Stafford, C. M.; Vogt, B. D.; Harrison, C.; Julthongpiput, D.; Huang, R. *Macromolecules* **2006**, *39*, 5095–9.
- (21) Nakajima, K. In *Polymer Physics from Suspensions to Nanocomposites and Beyond*; John Wiley & Sons: Hoboken, NJ, 2010; Chapter 3, p 129.
- (22) Liu, H.; Fujinami, S.; Wang, D.; Nakajima, K.; Nishi, T. *Macromolecules* **2011**, *44*, 1779–82.
- (23) Yabu, H.; Shimomura, M. *Chem. Mater.* **2005**, *17*, 5231–5234.
- (24) Stafford, C. M.; Vogt, B. D.; Harrison, C.; Julthongpiput, D.; Huang, R. *Macromolecules* **2006**, *39*, 5095–9.
- (25) Inoue, R.; Kanaya, T.; Miyazaki, T.; Nishida, K.; Tsukushi, I.; Shibata, K. *Mater. Sci. Eng., A* **2006**, *442*, 367–70.
- (26) Yang, Z.; Fujii, Y.; Lee, F. K.; Lam, C.; Tsui, O. K. C. *Science* **2010**, *328*, 1676–79.
- (27) Ahadian, S.; Ramón-Azcón, J.; Ostrovidov, S.; Camci-Unal, G.; Hosseini, V.; Kaji, H.; Ino, K.; Shiku, H.; Khademhosseini, A.; Matsue, T. *Lab Chip* **2012**, *12*, 3491–503.
- (28) Harrison, B. S.; Atala, A. *Biomaterials* **2007**, *28*, 344–53.
- (29) Namgung, S.; Kim, T.; Baik, K. Y.; Lee, M.; Nam, J.-M.; Hong, S. *Small* **2011**, *7*, 56–61.
- (30) Ahadian, S.; Ramón-Azcón, J.; Ostrovidov, S.; Camci-Unal, G.; Kaji, H.; Ino, K.; Shiku, H.; Khademhosseini, A.; Matsue, T. *Biomed. Microdevices* **2013**, *15*, 109–15.
- (31) Yuan, B.; Jin, Y.; Sun, Y.; Wang, D.; Sun, J.; Wang, Z.; Zhang, W.; Jiang, X. *Adv. Mater.* **2012**, *24*, 890–6.
- (32) Feinberg, A. W.; Feigel, A.; Shevkoplyas, S. S.; Sheehy, S.; Whitesides, G. M.; Parker, K. K. *Science* **2007**, *317*, 1366–70.
- (33) Martinelli, V.; Cellot, G.; Toma, F. M.; Long, C. S.; Caldwell, J. H.; Zentilin, L.; Giacca, M.; Turco, A.; Prato, M.; Ballerini, L.; Mestroni, L. *Nano Lett.* **2012**, *12*, 1831–8.
- (34) Tian, B.; Liu, J.; Dvir, T.; Jin, L.; Tsui, J. H.; Qing, Q.; Suo, Z.; Langer, R.; Kohane, D. S.; Lieber, C. M. *Nat. Mater.* **2012**, *11*, 986–94.
- (35) Greco, F.; Fujie, T.; Ricotti, L.; Taccola, S.; Mazzolai, B.; Mattoli, V. *ACS Appl. Mater. Interfaces* **2013**, *5*, 573–84.
- (36) Okamura, Y.; Kabata, K.; Kinoshita, M.; Miyazaki, H.; Saito, A.; Fujie, T.; Ohtsubo, S.; Saitoh, D.; Takeoka, S. *Adv. Mater.* **2013**, *25*, 545–51.
- (37) Fujie, T.; Matsutani, N.; Kinoshita, M.; Okamura, Y.; Saito, A.; Takeoka, S. *Adv. Funct. Mater.* **2009**, *19*, 2560–8.
- (38) Ren, K.; Crouzier, T.; Roy, C.; Picart, C. *Adv. Funct. Mater.* **2008**, *18*, 1378–89.
- (39) Zhang, H.; Takeoka, S. *Macromolecules* **2012**, *45*, 4315–21.